ADCP observations of migration patterns of zooplankton in the Cretan Sea

Emmanuel Potiris[1,2], Constantin Frangoulis[1], Alkiviadis Kalampokis[1], Manolis Ntoumas[1], Manos Pettas[1], George Petihakis[1] and Vassilis Zervakis[2]

[1]Institute of Oceanography, Hellenic Centre for Marine Research, Heraklion, Crete, 72100, Greece

[2]Department of Marine Sciences, School of the Environment, University of the Aegean, Mytilene, 81132, Greece

Correspondence to: Emmanuel Potiris (mpotiris@hcmr.gr)

Abstract. The lack of knowledge of the mesopelagic layer inhabitants, especially of those performing strong vertical migration, is an acknowledged challenge as its incomplete representation leads to the exclusion of an active carbon and nutrient pathway from the surface to the deeper layers and reversely. The vertical migration of mesopelagic inhabitants (macro-planktonic and micro-nektonic) was observed by acoustical means in the epi- and mesopelagic layer of the open oligotrophic Cretan Sea (south Aegean Sea, Eastern Mediterranean) for almost 2.5 years at the site of an operational fixed-point observatory located at 1500 m depth. The observed organisms were categorized in four groups according to their migration patterns. The variability of the migration patterns was inspected in relation to the physical and biological environmental conditions of the study area. The stratification of the water column does not act as a barrier for the vertical motion of the strongest migrants, moving up to 400 m every day. Instead, changes of light intensity (lunar cycle, daylight duration, cloudiness) and the presence of prey and predators seem to explain the observed daily, monthly and seasonal variability. The continuous presence of these organisms, yet capable of vertical motion and despite the profound seasonal circulation variability at the site of the observatory, implies their presence in the broader study area. The fundamental implications of the above for biogeochemical processing in oligotrophic seas due to the intimate link of the C and nutrient cycles, are discussed.

1 Introduction

The biological organic carbon pump is the major oceanic process that photosynthetically converts the dissolved CO_2 in the surface layers of the ocean to particulate organic carbon, which is then consumed by pelagic biota, and exported to depth by a combination of sinking particles, advection or vertical mixing of dissolved organic matter and transport by animals (Turner, 2015). Buesseler and Boyd (2009) have noted that ‘‘the surface ocean’’ is ‘‘where the ‘strength’ of the biological pump is set’’ whereas ‘‘the subsurface ocean’’ is ‘‘where the ‘efficiency’ of the biological pump is determined.’’

The main factor determining the biological pump’s efficiency in the mesopelagic and bathypelagic zones, is the organic carbon export done by sinking and vertical migration by zooplankton and fish, together with microbial degradation. The diel vertical migration (DVM) of zooplankton, i.e. their vertical movement in the water column within the 24-h day, creates an active flux, pumping carbon between epipelagic and mesopelagic layers (review by Turner, 2015). This DVM of zooplankton has as its most common pattern a single descent to maximum depth during daytime, and a single ascent at minimum depth during night-time (review by Cohen and Forward, 2009). DVM is a behavioural response that has been related to several exogenous (light, temperature, salinity, oxygen, hydrostatic pressure, stratification) and endogenous (sex, age, state of feeding, biological rhythm) factors (review by Forward, 1988; van Haren 2014, and references therein). Light has emerged as the major external factor controlling DVM behavior (review by Cohen and Forward, 2009), although insufficient to explain some cases where DVM occurs at depths larger than 1000 m, where light cannot penetrate (van Haren 2014, and references therein).

There are still gaps of knowledge regarding midwater depths which severely limit our ability to quantify the efficiency of the biological pump (Robinson et al., 2010). Concerning zooplankton DVM, one of the methodological limitations, is that

the populations of large individuals (macrozooplankton) belonging to important and common predatory groups capable of strong migrations, such as the chaetognaths, amphipods, euphausiids, decapods, have been underestimated, as many of them escape the standard 200 μm mesh size net when towed at the recommend speed of less than 1 m s^{-1} (Moriarty and O'Brien, 2013). However, such large individuals can be detected by low frequency Acoustic Doppler Current Profilers (ADCPs hereafter).

Progress in ocean acoustics and marine technology during early 1980s (Holliday, 1977; Holliday and Pieper, 1980; Holliday et al., 1989; Costello et al., 1989) allowed the estimation of distribution patterns and biomass of zooplankton and micronekton to be inferred from ADCPs (Flagg and Smith, 1989). To measure currents, ADCPs transmit sound pulses in different directions. The sound is scattered by particulate matter in the water column, and radial velocities are computed from the Doppler shift of the backscattered signal (Gordon, 1996). The intensity of the backscattered sound can also be used in conjunction with net samples for estimating the biomass of zooplankton (Ashjian et al., 2002). Although the estimated ADCP backscatter is a by-product (Bozzano et al., 2014) and thus more suitable for qualitative than quantitative analysis (Brierley et al., 1998), field studies complemented with ADCP-derived sound scattering have been used to describe biological patterns in the interior of the ocean, such as zooplankton aggregations (Zhou and Dorland, 2004) and vertical migration (Postel et al., 2007) with remarkable detail.

In the Mediterranean Sea, there have been several studies on vertically migrating zooplankton (see table 5 in Andersen et al., 2001) and some have shown a substantial contribution to total carbon export in deep waters by the active transport of migrants (Isla et al., 2015, and references therein). However, these Mediterranean DVM studies have been mainly based on net sampling for short total sampling periods (e.g. discontinuous sampling at monthly frequency or continuous sampling for a few weeks). It is worth noticing that studies of macrozooplankton are less than of mesozooplankton, and that even for mesozooplankton there are very few interannual scale studies in the open Mediterranean Sea (Siokou-Frangou et al., 2010). Among the Mediterranean DVM studies, the majority has been made in Western Mediterranean (see table 5 in Andersen et al., 2001; review by Saiz et al., 2014). These studies have pointed out different migrating strategies depending on species, with some species migrating upwards and other downwards at night, as well as a within species age-depth and sex-depth differential distribution. These observations were made in both the Eastern and Western Mediterranean (Fragopoulou and Lykakis, 1990; Andersen et al., 2001). The only DVM study in the Cretan Sea (Heraklion Bay) upper slope (300 m seabottom) studied near-bottom macrozooplankton, and reported a reversed DVM, i.e. downward migration during night (Koulouri et al., 2009).

The Cretan Sea is the most voluminous and deep (2500 m) basin of the Aegean Sea and an area of intense mesoscale variability and multiple scale circulation patterns. Two mesoscale gyres form a dipole in the Cretan Sea (Theocharis et al., 1999; Cardin et al., 2003; Kassis et al., 2015), while it is also an area of intermediate and/or deep-water formation (review by Skliris et al., 2014). Such areas of water formation are key locations for monitoring of the Mediterranean biochemical functioning (Malanotte-Rizzoli et al., 2014). Modelling studies have shown that the open Cretan Sea's biochemistry is representative of a wide area of the Eastern Mediterranean varying from 0.6-1.6 x 10^6 km^2 depending on the variable (i.e. PP, SST, pH, O_2, NO_3, Chl-α) (Henson et al., 2016).

Satellite (SeaWiFS) studies of chlorophyll-α (Chl-α) have clustered the Cretan Sea in a wider bioprovince of the South-Central and Eastern Mediterranean that covers 60% of the total Mediterranean area, characterized by generally oligotrophic conditions (D'Ortenzio and Ribera d'Alcala, 2009). The presence of a Deep Chlorophyll Maximum (DCM hereafter), a common Mediterranean feature, which deepens going eastwards (e.g. Lavigne et al., 2015), also characterises the Cretan Sea and depends on a close coupling of biological and physical processes. In fact, although the DCM's magnitude is mainly determined by biological mechanisms, the DCM depth and structure are essentially determined by optical-physical factors (e.g. Mann and Lazier, 2006; Varela et al., 1994; Crise et al., 1999). In the Cretan Sea the vertical extent and the intensity of the mesoscale gyres forming a dipole govern to a large extent this coupling (Petihakis et al., 2002).

Zooplankton studies in the Cretan Sea, were all done only on mesozooplankton (Mazzocchi et al., 1997; Siokou-Frangou et al., 1997; Siokou et al., 2013), with only one study on near-bottom macrozooplankton (Koulouri et al., 2009). Mesozooplankton abundance in the Cretan Sea's epipelagic layer was found to be at the same level as in the open Ionian and Levantine and community composition have shown significant similarities with the above areas (Siokou-Frangou et al., 2010 and references therein). Regarding deep living zooplankton, less is known for the Eastern Mediterranean (review by Saiz et al., 2014), although deep living mesozooplankton stock and composition has been investigated (Siokou et al., 1997, 2013) and its importance in consuming sinking particles reported (Koppelman et al., 2004). For deep living macrozooplankton there is even less information. The euphausiid species found in the whole Mediterranean Sea are the same, however the predominant ones are different in the eastern basin and Thyrrenian Sea, than those found in the western basin west of the Thyrrenian Sea (Wiebe and Abramo, 1972).

ADCP studies of DVM the Mediterranean have been limited. In the central Ligurian Sea, Bozzano et al. (2014) used an upward looking ADCP positioned at 100 m depth. They found that the main migration pattern is the daytime migration, and also, that deeper and stronger migration ranges are encountered during winter. In the Alboran Sea, van Haren (2014) with an upward looking ADCP positioned at approximately 800 m depth, found DVM to be related with internal waves. To our knowledge, there has been no ADCP study of DVM in the Eastern Mediterranean. However, during a study of the current velocities in the Cretan Sea back in 2000, Cardin et al. (2003) using an ADCP (75 kHz), reported a noise in the measurements of vertical velocity, and migrating zooplankton was given as a possible explanation.

The present study was stimulated by this hypothesis by Cardin et al., and knowing that for the 75 kHz frequency objects with size of 5 mm (1/4 of transmit pulse wavelength) or more reflect sound, thus causing a strong backscatter signal (Thomson and Emery, 2001). Following this hypothesis, four consecutive deployments of the same 75 kHz ADCP and at the same location as Cardin et al., covering a period of two and a half years, provided a unique opportunity to study the migration patterns of zooplankton, continuously and in high frequency, for a long period in relation to environmental conditions. The aim of this paper is to present the observed distribution patterns of zooplankton (focusing on DVM) and discuss their relation to physical and biological environmental conditions, such as daylight, currents, stratification and food resources.

2 Materials and methods

2.1 Experimental setup

The Poseidon E1-M3A observatory (www.poseidon.hcmr.gr) is located at 25.12° E, 35.74° N in the center of the Cretan Sea at a depth of 1500 m (Figure 1, a). It consists of two moorings: the first one has a surface buoy and a real-time multi-sensor array down to 1000 m, while the second is a subsurface one, hosting an upward looking RDI 75 kHz ADCP. The observing effort is complemented by monthly R/V cruises to perform CTD casts (temperature, salinity, fluorescence) and net tows (zooplankton). The ADCP data set used in the present study consist of four successive deployments of variable duration, which extended over a period of two years and six months, from 15 November 2012 to 20 May 2015 (Table 1). The distance between the ADCP mooring line and E1-M3A buoy varied slightly but it was less than 2.7 NM for all deployments (Figure 1, c). The primary purpose for the ADCP deployment was to study currents. The first deployment was considered as a test of the setup, so the sampling scheme and the depth of the ADCP were selected empirically (Table 1). The first deployment confirmed the feasibility of monitoring biological activity and it became obvious that a greater depth should be chosen, since the parking depth of zooplankton was deeper than the initial ADCP deployment depth and the sea surface reflection contaminated the first 50 m of the water column. However, the rearrangement of the mooring line was not possible due to the tight schedule of the next two deployments, and thus, only the last ADCP deployment was about 120 m deeper than the previous ones.

The ADCP sampling plan was optimized in terms of temporal and spatial resolution by setting different sampling schemes at each deployment (Table 1; Figure 1, b). The aim was to check the consistency of the vertical velocity measurements of zooplankton and backscatter coefficient (defined in Sect. 2.2) between deployments. No significant differences in the vertical velocities and the backscatter coefficient between deployments of variable cell length and sampling rate, is an indication of reliable – accurate measurements. Thus, it is possible to identify biases caused by the sampling scheme, instead of the velocity errors due to the ADCP accuracy and of the backscatter coefficient estimation methodology.

One parameter used to potentially identify the optimal cell extension and sampling interval for the most appropriate recording of zooplankton signals was the hereafter defined *burst speed*. The burst speeds of each cell are defined as the highest and lowest vertical velocity measurements respectively during a time period of one day. The velocity measurement inside a cell over the sampling interval is the result of the averaging of several pings. As the recording interval increases, the cell extension decreases and the actual zooplankton speed increases, we expect the actual zooplankton speed to be underestimated because zooplankton will not be inside the cell throughout the duration of the measurement but only during a fraction of it. The largest underestimation is expected when the actual zooplankton migrating speed is maximum. Thus, comparison of upward and downward burst velocities between deployments at depths around 250 m (the depth at which the highest migrating speeds were recorded) were used to identify the most appropriate sampling scheme.

The challenge was to identify the lowest sampling rate that would still give acceptable resolution of the ascending/descending zooplankton movement, while conserving power and extending the deployment period as much as possible. Two sampling and averaging intervals, of lengths 30 min and 1 hour respectively, were tested in order to select the optimum sampling scheme. During the first deployment, a sampling interval of 30 min was used, to be followed by a 1 h interval during the second deployment. Comparison of the data from the two deployments revealed an underestimation of burst migrating velocities during the second data set (Figure 2, a & b) because of the lower sampling rate (1 h), thus the initial value of 30 min was selected for the last two deployments.

The range of the cells used (10 m – 20 m), on the other hand, did not affect the burst speed and the average velocity measurements. Based on visual inspection, smaller cell extension during the 1st, 3rd and 4th deployments (30 min sampling interval) did not result in smaller burst and average speeds. However, using a small bin size (10 m) during the last deployment resulted in noisy velocity measurements. The depth-integrated S_v (backscatter coefficient, defined in Sect. 2.2) between the depths observed at all deployments were also consistent. The seasonal variability of the physical properties of the water column affected the estimation of S_v at depths shallower than 100 m, mostly during late August. Placing the ADCP at an upward looking position at a smaller depth than the nominal range resulted in erroneous data of the first 50 m of the water column due to sound reflection on the sea surface.

2.2 Data processing/analysis and visualization of backscatter data

The backscatter coefficient S_v[dB re (4π m^{-1})] is given as:

$$S_v = C + 10\log_{10}\left((T_x + 273.16)R^2\right) - L_{DBM} - P_{DBW} + 2aR + K_c(E - R_r), \quad (1)$$

where C[dB] $= -159.1$ is an instrument constant, T_x[°C] the transducer temperature, R[m] the slant range, L_{DBM} the $10log_{10}$ of the transmit pulse length [m], P_{DBW} the $10log_{10}$ of the transmit power [W], a[dB m^{-1}] the sound absorption coefficient, K_c a constant of proportionality for converting the incoming raw echo data to dB, $E[counts]$ the raw echo data and $E_r = \min(E)$[counts] the reference raw echo per transducer when there is no signal. S_v was calculated according to Deines (1999), K_c according to Heywood (1996), the speed of sound for the calculation of R according to Gordon (1996) and a according to Ainslie and McColm (1998).

Instantaneous vertical velocity profiles were depth averaged and split in daily datasets to identify the hours of the day during which the zooplankton moves upward or downward, as well as the seasonal and interannual variability in the

ascend/descend hours. Another step was to select the maximum and minimum vertical velocities of each daily piece of data during the time of the upward and downward movement. Depending on the sampling rate, two to four samples were averaged. At last, histograms of vertical velocity versus depth one hour before and one hour after sunrise/sunset times were used to identify possible ascending/descending differences of migration patterns and evaluate the consistency between the different ADCP sampling schemes.

Climate Data Operators (CDO, 2018), Ocean Data View (Schlitzer, 2016) and Generic Mapping Tools (Wessel et al., 2013) were used for the data processing and visualization. Wind stress and sensible/latent fluxes were computed from the quality-controlled buoy data with the air-sea toolbox to identify the time when conditions favor overturning of the water column (http://woodshole.er.usgs.gov/operations/sea-mat/air_sea-html/index.html).

2.3 Description and processing of auxiliary data

To estimate volume backscattering, assess environmental conditions during deployments and assist interpretation of ADCP measurements, several complementary data sets have been used (Table 2).

The E1-M3A buoy measures meteorological variables (wind speed, gust and air temperature were used here) as well as temperature, conductivity and fluorescence at multiple depths (20, 50, 75 and 100 m). Temperature and conductivity measurements are also available at the sea surface and at 250 m depth. The chlorophyll concentrations are measured with the WETLABS ECO FLNTU fluorescence sensors which are mounted on the moored 16plus CTDs. A downward looking Nortek 400 kHz ADCP is mounted to the buoy hull, measuring horizontal currents at 5 m bins from the surface down to 50 m depth. Due to the lack of compatibility of the 400 kHz ADCP with the buoy software, backscatter measurements are not available from this instrument. The above meteorological and marine surface parameters were downloaded from the Poseidon on-line database (www.poseidon.hcmr.gr), where they are stored in real-time. In addition, due to occasional problems with the real-time underwater transmission, subsurface sensor data were downloaded from the memory logs of the instruments during the regular bi-annual maintenance. Meteorological and sea surface measurements from the buoy's sensors span a period of 24 months (from 22 May 2013 to 25 May 2015) and subsurface measurements a period of 20 months (from 22 May 2013 to 10 January 2015). Buoy data have undergone automated quality control, such as rejection of stalled values and application of min-max and spike filters. Visual inspection was the last quality control step; the remaining suspect measurements were removed manually. The heat flux through the air-sea interface computations were based on the air-sea interaction Matlab routines provided by Rich Pawlowitz (via the SEAMAT collection, https://sea-mat.github.io/sea-mat/), applied on the E1-M3A meteorological and sea-surface data.

2.4 Limitations

Several limitations of the ADCP and auxiliary data should be carefully considered. S_v is a proxy for zooplankton biomass and when integrated along the acoustical beams it can provide a gross measure of the instantaneous biomass of the water column (changes in the acoustical character of zooplankton cannot be identified). Although the integrated S_v is consistent among the deployments (discrepancies between deployments were observed only for the first few bins), such an analysis is not meaningful with the experimental configuration of this study, since the zooplankton is not permanently in the range of the ADCP and because of the seasonal succession of dominant species constituting the zooplankton stocks in the Cretan Sea (Gotsis-Skretas et al., 1999). The upper 50 m of the water column are not measured, thus the depth integrated S_v exhibits significant variability due to the monthly change of the depth at which zooplankton ascends during night-time because of moonlight. Also, the whole deep scattering layer is found inside the ADCP range only for a small period of the 4th deployment, adding another source of variability that is not attributed to biomass changes of zooplankton. Another source of error, which largely depends on the availability of auxiliary data, is the imperfect calculation of the effects of the gradients of the upper

water column in the estimation of S_v due to the changes in temperature and salinity. The above problems are generally encountered when measuring zooplankton with upward looking ADCPs and should be treated with caution in acoustical studies of zooplankton.

2.5 Hydrology of the Cretan Sea

The ADCP site is located at the center of the semi-permanent dipole of the Cretan Sea, which consists of a cyclone to the east and an anticyclone to the west of the observatory (Theocharis et al., 1999; Korres et al., 2014). Low frequency variability at the study site is controlled by the intensity and the vertical extent of the dipole as reported by Cardin et al. (2003). Four water masses fill the surface and subsurface layers of the Cretan Sea. Modified Atlantic Water (MAW, S=38.5-38.9 psu) fills the 20 m - 100 m layer. Cretan Intermediate Water and Levantine Intermediate Water, that have similar characteristics (CIW & LIW, θ=14.9-15.1 °C, S~39-39.1 psu) fill the 200 m - 500 m layer. Transitional Mediterranean Water (TMW, θ=14.2 °C, S=38.92 psu), a mixture of Levantine Intermediate Water and Eastern Mediterranean Deep Water enters through the Cretan Straits and its core lies at the 500 m - 800 m layer (Georgopoulos et al., 2000; Velaoras et al., 2013) or deeper (Velaoras et al., 2015). Below TMW lies the Cretan Deep Water, a water-mass argued to have local (Theocharis et al., 1999) or North/Central Aegean origin (Zervakis et al., 2000; Gertman et al., 2006). Inflow of Atlantic water (Theocharis et al., 1999), typically during late summer, causes a salinity minimum at the subsurface layer.

3 Results

3.1 Environmental conditions at the study site

Sea surface temperature ranged seasonally from 15 ºC to 26 ºC and salinity ranged from 38.8 psu to 39.5 psu (Figure 3, b, c). The salinity of the deeper layers ranged from 38.9 psu to 39.1 psu. Lowest temperatures were observed during February and March, while highest temperatures during August and September. The seasonal cycle of temperature penetrated down to 100 m and the permanent thermocline extended down to 350 m (Figure 3, b). Salinity also exhibited a seasonal cycle down to 100 m but the seasonal signal dominated salinity variations of the upper part of the water column (Figure 3, c). Largest salinity values were observed during calm, cloud free summer days. A salinity minimum between surface and 100 m depth was also observed in Figure 3, c. Deep casts (Figure 3, e & f) revealed a continuous change of the water column towards fresher and colder values between 250 and 1000 m especially from 2012 to 2016, which points to intensified horizontal motion of the subsurface layers. The temperature at the depth of the deep scattering layer around 450 m (based on the available data set; Figure 3, d, e & f), ranged from 14.55 °C to 14.9 °C and the salinity from 38.98 psu to 39.04 psu.

At the study area, prevailing winds blew from N-NW (Figure 4, a). Short-term variability of air temperature during winter was larger, due to strong northerly winds, which caused the air temperature to drop below 10 ºC. Latent heat loss typically ranged between 100 W m^{-2} and 200 W m^{-2}. Sensible heat flux also resulted in net loss, but it was negligible from March to October. During the rest of the year typical values were less than 50 W m^{-2}. Sensible heat loss contributed significantly to the flux budget when wind stress became larger than 0.2 Pa (average wind stress of the complete data set was 0.82 Pa). Wind stress during December of 2013 was more than 0.2 Pa on average, while peak values of 0.8 Pa were also observed. Consequently, the monthly average sensible heat flux was about 100 W m^{-2} and peak values were about 300 W m^{-2}. Latent heat during that period peaked at 600 W m^{-2}. Similar atmospheric conditions that favoured convection of the upper 100 m of the water column were observed during 10 to 22 February 2015.

Average water velocity from surface down to 50 m was 0.29 m s^{-1} towards S-SE and is invariant with depth. The layer between 50 m and 350 m depth was characterized by a diminishing vertical shear that was largest between 50 m to 150 m

depth and vanished below 400 m (Figure 4, d, where only the fourth deployment is displayed, since in previous deployments the larger bin size caused underestimation of the high vertical wavenumber shear). The average current speed below the depth of 350 m was 0.06 m s^{-1}. The direction of the axis of maximum variance between the surface and 50 m was S-SE and gradually turned to S-SW at 200 m depth. Currents were less unidirectional with depth too. The strong currents of the surface layer exhibited the least directional variability (Figure 4, b & c). High frequency variability at the site consisted of inertial and tidal currents, which accounted for a small portion of the total variance (less than 8%), even though the inertial motions were dominant over short periods.

During the study period the core of DCM was observed between 70 m and 120 m and its vertical extent was around 60 m (Figure 5, a). On average, the largest chlorophyll values were observed at the 75 m and 100 m sensors of the buoy (Figure 5, b). Also, at these depths, the short-term variability was comparable to the variability due to the annual cycle, while for the 20 m and 50 m sensors the seasonal variability was dominant. The DCM formed from February to April and was usually destroyed by October (see changes of the depth range for which chlorophyll concentration is above 70% of the maximum value in Figure 5, a).

3.2 Scattering and migrating groups of organisms

The results of the four ADCP deployments of a total duration of 2.5 years (Figure 6) provided a wealth of information about the scattering organisms and their movement in the water column. Characteristics that are easily visible in Figure 6 include the presence of a deep layer of scatterers (unfortunately visible only in the last deployment, since only then was the ADCP placed deep enough to record it), a seasonal and a monthly (moon) cycle.

A closer examination of daily backscatter patterns (Figure 7), allowed the categorization of the scattering organisms in four groups according to their migration patterns, on the basis of distinguishable trails of volume backscatter measurements of the ADCP. Three of them exhibited a daily migrating pattern, while the fourth remained at a constant depth. The first group (group A hereafter) did not migrate. It was found at 400 m - 450 m, and it formed a deep scattering layer (Figure 7, c).

Group B (Figure 7) followed the normal DVM pattern i.e. it moved close to the surface at dusk and returned to the parking depth at dawn where it stayed during the day. This group spent the day-time at 400 m - 450 m depth and the night-time between 150 m and surface (Figure 7). When at the bottom of the seasonally varying day-time parking layer (60 - 160 m), its vertical velocity decreased, while still moving towards the surface. The bottom of the day-time parking layer was identified by the deceleration of upward movement and subsequent increase of S_v (Figure 7), as the zooplankton spent more time in a particular cell when moving at smaller speed. The change of depth of the bottom of the day-time parking layer of group B was in good agreement with the time variation of the depth of maximum chlorophyll concentration.

The backscatter coefficient at any certain depth, as long group B was above that depth, was larger during night-time compared to day-time (Figure 7). The exception to this rule was the deep scattering layer. The result was the "curtain" shape of S_v seen in Figure 7, which implies that a part of zooplankton that forms group B spread in the entire 50 m - 400 m water column while migrating. The smallest S_v values, close to the system noise floor, were observed between 250 - 300 m, when group B was found at the parking depth.

Between the depth of 300 m and 350 m, S_v never fell close to the noise floor (Figure 7, c), even in the absence of group B during day-time, pointing to the presence of scatterers and thus to a third group of organisms (group C hereafter). Group C migrated from 350 m to 300 m or from 250 m to 200 m depending on the period of the year.

At shallower depths a fourth group was observed (Figure 7, Group D), which spent most of the day-time in a depth of 180 m - 240 m and during the night it moved to more shallow depths of 60 m - 90 m, where its trails met with those of group B. This was close to the depth where the layer with the largest concentration of phytoplankton throughout most of the year was observed. Its backscatter signal was not as strong as that of group B. Actually, its trail was easily distinguishable mostly during

the time of its upward motion, as a secondary thin strong S_v trail, shallower than the one caused by group B, and less during the downward motion (Figure 7). This signal was present at all deployments, but not throughout each deployment, and its characteristics, such as depth and slope, were consistent between deployments.

3.3 Migration timing, duration and velocity

The duration of strong migration did not change with time, with two hours spent each way (four hours in total) (Figure 8, a). Descend was symmetrical with respect to the sunrise. It started one hour before and ended one hour after the sunrise (Figure 8, a). Ascend started half an hour before and ended one and a half hour after the sunset (Figure 8, b). Depth-averaged velocities during strong migration time were about 3 cm s^{-1}. While the duration of the strong migration was constant, the migrating velocity changed seasonally, following the duration of day which, at 35° longitude, lasts 9.8 h on winter solstice and 14.5 h on summer solstice, as is clearly shown in Figure 8, b, despite the fact that they are quite noisy. Downward velocity was slightly larger than the upward velocity by almost 1 cm s^{-1} on average (Figure 8, b).

Monthly variability was observed at the depths at which strong downwards migration started (speeds higher than 2.5 cm s^{-1}) (Figure 9). Also, in Figures 9 and 10 it can be seen that zooplankton did not migrate at a constant velocity with depth. Highest upward velocities, close to 6 cm s^{-1} were recorded between 200 m and 300 m. Highest downward velocities were recorded between 250 m and 350 m (Figure 10). Since Group B travelled the largest distance in the course of a day, the largest vertical velocities recorded, especially between 200 m and 350 m, might be due to the migration of group B. At the depth of 200 m the ADCP recorded relatively small vertical velocities, about 2 cm s^{-1} (Figures 9 & 10, all panels), which distorted the vertical profile that would be expected by group B, unless group B decelerated at the bottom of the photic zone. The dispersion of the vertical velocity around the average value at that depth was much less than all the other depths (Figure 10, all panels).

It was not possible to distinguish the velocity of group B from the velocity of group C, as their S_v trails overlapped during migration. However, utilizing the S_v trails attributed to groups B and D it was possible to distinguish the velocity of group D. The time average vertical velocities and S_v relative to sunrise and sunset hours showed that secondary peaks of S_v attributed to group D were accompanied by a small increase in vertical speed (Figure 11, all panels). According to the time average velocity measurements in Figure 10, a & b, group D migrated at an average velocity of about 0.2 cm s^{-1}. The migrating velocity of group D calculated indirectly using the trails of S_v (Figure 11, c & d) was about 0.4 cm s^{-1}. The depth averaged migrating velocity of 3 cm s^{-1} recorded by the ADCP and attributed to group B was consistent with the indirect calculation of the migrating speed of this group based on the distance travelled and the duration of its migration (about 3.5 cm s^{-1}).

3.4 Effect of an extreme meteorological event

Three successive events of harsh weather conditions were observed from 10 to 13, from 17 to 21 and from 23 to 25 February 2015. The sky was mostly overcast (Figure 12, a), air temperature dropped at 7.5 $^{\circ}$C (Figure 12, b), wind speed reached 15 m s^{-1} and wind gust exceeded 20 m s^{-1} (Figure 12, c). The third event was shorter than the first two and caused an increase in air temperature. The homogenization of the water column prior to the first event did not exceed the 50 m (as shown from the E1-M3A time series) while the nearest in time available CTD cast on the 3rd of March revealed that the first 100 m of the water column were then homogenized. The zooplankton was distributed from the surface down to 350 m all day long (Figure 12, e), especially during the first two events, although S_v remained larger during night-time compared to day-time above the depth of 300 m. Also, only small migrating velocities were measured especially during the first two events (Figure 12, d). During the second event, the core of the deep scattering layer moved shallower at the depth of 350 m. After the third event, the pattern of the backscatter coefficient above 300 m returned back to the "normal" conditions, but the deep scattering layer remained generally shallower and moved coherently in the vertical direction from 450 m to 350 m until the 2nd of April

(Figure 12, e). Thus, changes at the deep scattering layer were observed, which is found well below the maximum depth at which the overturning took place.

4 Discussion

4.1 Factors affecting zooplankton migration

DVM of zooplankton has been related to several exogenous and/or endogenous factors (review by Ringelberg, 2010). In the present study, light intensity seemed to be the major factor affecting the zooplankton migration on daily, monthly and annual time scales. Light can act as an endogenous (entraining circadian rhythms) or exogenous factor controlling DVM. Several hypotheses attempt to explain the exogenous role of light. According to the rate-of-change hypothesis, the variation in relative rate and direction of change in light intensity is the cue to initiate DVM, whereas light acts also for orienting and controlling DVM (Cohen and Forward 2009).

A scenario that has been proposed to explain DVM is that of a photobehaviour formed in order to avoid the damaging effect of solar ultraviolet (UV) radiation. The UV photoreceptors found on zooplankton have supported this (Williamson et al., 2011). However, this mechanism fails to explain the maximum depth of DVM in our case, since UV radiation in the eastern Mediterranean reaches its maximum value at a depth of 50 m (Tedetti and Sempéré, 2006).

Another approach to explain DVM proposes a photobehaviour attempting to balance the need of feeding, while avoiding visual predators. Therefore, DVM as a photobehaviour should consider the rate of change of light combined with the rate of change of food abundance and kairormones (released by predators and detected by zooplankton). In order to maximize the detection of downwelling light, DVM organisms have adapted their maximum visual sensitivities to wavelengths of about 450 - 470 nm (although species with photosensitivity in wavelengths larger than 470 nm sensitivity have been reported as an additional adaptation to bioluminescent emissions) (review by Cohen and Forward 2009).

According to the results presented here, during full moon the zooplankton prey almost 50 m deeper than during the new moon, a possible behavioral response to increased light conditions. Twilight effects on DVM using data from a downward looking 300 kHz ADCP measuring from the surface down to 80 m were also reported by Bozzano et al. (2014) in the Ligurian Sea.

Changes in migration depth and speed were also correlated to cloudiness. Amplitude changes of the extent of DVM due to changes in cloudiness can also be found in the results of Pinot and Jansá (2001). Cloudiness may have an indirect effect on migrants, since the phytoplankton production, and thus the available prey concentration, becomes lower under lower light conditions. In addition, the prey is spread downward due to convection. Thus, the migrants have to spread in a larger water column in order to obtain a sufficient amount of prey.

Another factor that seemed to affect migration was Chl-α concentration and location. The seasonally varying zooplankton day-time parking layer extended from the surface down to a maximum depth of 160 m. The bottom of the day-time parking layer was found at an average depth of 100 m. It was recorded deeper from May to July and shallower from November to January. The upward motion of the migrating groups decelerated at the depth of the largest chlorophyll concentration. The largest vertical velocities were recorded during spring, when the seasonal pycnocline started to form. This was the period of the year that the phytoplankton (Chl-α) was spread quite homogeneously throughout the upper 160 m of the water column and the DCM was not formed yet.

The fact that the parking depth of the migrating zooplankton groups B and C (which is also the parking depth of the non-migrating group too) is found so deep (450 m), cannot be explained by light, phytoplankton prey concentration (since these are zero below 200 m), nor by a temperature, salinity or density gradient at that depth. Considering that at the parking depth of these groups the vertical shear practically vanishes, and the horizontal currents are the weakest ones recorded, it might

indicate an active behavioral adaptation to minimize energy loss by maintaining their position at a depth with minimum turbulence.

4.2 Zooplankton sampling considerations

Local literature does not allow us to clearly identify the taxonomic composition of the migrating assemblages found in the present study. The few published studies that have sampled zooplankton in the epipelagic and mesopelagic layer of Cretan Sea, were all done with vertical hauls (≈ 1 m s^{-1}) of 200 μm mesh size nets (Mazzocchi et al., 1997; Siokou-Frangou et al., 1997; Siokou et al., 2013) and are ongoing similarly during the monthly monitoring program at the E1-M3A observatory. Thus, they are inappropriate to capture organisms at the size of 5 mm, which are the smaller organisms expected to contribute significantly to the backscatter of a 75 kHz ADCP. It is however clear that the assemblages examined in our study include organisms other than copepods, since the biggest copepods species reported in the area (Mazzocchi et al., 1997; Siokou-Frangou et al., 1997; Siokou et al., 2013) reach a maximum size of ≈ 3.5 mm (Razouls et al., 2005 – 2018). The only qualitative indication about the nature of these migrators in the Cretan Sea is one tow made above the ADCP in December 2013, that captured large organisms (larger than 5 mm) from which known migrators were decapod larvae, euphausiid larvae, siphonophores and chaetognaths. Indications can also be given by studies targeted on zooplankton migrators in the Western Mediterranean Sea by Andersen and collaborators (Andersen and Nival, 1991; Andersen and Sardou, 1992; Andersen et al., 1992; Sardou et al., 1996). Among the several migrant species reported, the most abundant ones that were present all year round (euphausiids, siphonophores and decapods) were concentrated above 150 m at night-time, whereas during day-time the depth of their maximum abundance was found seasonally variable (between 300 m and 500 m) (Sardou et al., 1996). These groups appeared to have similar behavior to group B in the present study. Small euphausiids migrated from 420 m to 240 m, whereas non-migrants remained below 300 m (Sardou et al., 1996), with similar behavior to groups C and A respectively in the present study.

The above work reveals a significant problem associated with the in situ sampling of the above mentioned zooplanktonic groups. Considering that the clear majority of samplings in the area take place during day time, above 100 m depth (when groups A, B, C, D are at the deeper parts) and with inappropriate net type and tow to capture large organisms (as explained above), it is rational to assume that they are misrepresented in the samples. Appropriate sampling strategy with day and night sampling regularly (monthly frequency) with appropriate net type and tows to study diel and seasonal variation of large organisms, has been done in few locations such as the Ligurian Sea (Sardou et al., 1996), the ALOHA site (Al-Mutairi and Landry, 2001) and the BATS site (Madin et al., 2001; Jiang et al., 2007), with significant logistical effort.

4.3 Implications for biogeochemical cycles

If large stocks of large zooplankton actively migrate over significant vertical distances, in an oligotrophic deep system such as the Cretan Sea, then, new carbon pathways will have to be included in our models, reconsidering the energy flow and the dynamics of the system. In fact, since the carbon inflow (feeding) to the migrant groups comes from lower trophic levels (i.e. phytoplankton) at the euphotic zone, the zooplankton migrators may cause an important active downward vertical flux of matter, thus increasing the biological pump's efficiency (review by Frangoulis et al., 2004). The gaps of knowledge for midwater depths severely limits our ability to quantify the efficiency of the biological pump (Robinson et al., 2010). In the Cretan Sea, the lack of knowledge of the role of zooplankton DVM and the functioning of the whole mesopelagic ecosystem may constitute an important knowledge gap of the biological pump's efficiency in the area that requires exploration. Additionally, the observed patterns are expected to have significant implications in the system dynamics particularly if one considers the oligotrophic character of the Cretan Sea. The observed DVM is expected to act as a transfer mechanism of organic matter (carbon and nutrients) from the euphotic zone to the deeper parts of the water column, overcoming the physical

barrier of the pycnocline. This active flux of matter may occur since the DVM speeds recorded (larger than 3 cm s^{-1}) were higher than reported zooplankton faecal pellet sinking speeds (higher than 1 cm s^{-1} for euphausiids - review by Frangoulis et al., 2004). This mechanism will enhance the oligotrophism of the mesopelagic layer since there are no effective mechanisms of very deep-water mixing and there is a strong decoupling of the surface layers with the deeper parts of the water column. Thus, the surface layers are deprived of important nutrients, although in the actual nutrient budget one has to take into account other parameters such as zooplankton excretions at the surface layers etc.

Acknowledgements

Part of the work has been funded by JERICO-NEXT project. This project has received funding from the European Union's Horizon 2020 research and innovation programme under grant agreement No 654410.

References

Ainslie, M. A. and McColm, J. G.: A simplified formula for viscous and chemical absorption in sea water, J. Acoust. Soc. Am., 103(3), 1671–1672, doi:10.1121/1.421258, 1998.

Al-Mutairi, H. and Landry, M. R.: Active export of carbon and nitrogen at Station ALOHA by diel migrant zooplankton, Deep Sea Res. Part II Top. Stud. Oceanogr., 48(8–9), 2083–2103, doi:10.1016/S0967-0645(00)00174-0, 2001.

Andersen, V. and Nival, P.: A model of the diel vertical migration of zooplankton based on euphausiids, J. Mar. Res., 49(1), 153–175, doi:10.1357/002224091784968594, 1991.

Andersen, V. and Sardou, J.: The diel migrations and vertical distributions of zooplankton and micronekton in the Northwestern Mediterranean Sea. 1. Euphausiids, mysids, decapods and fishes, J. Plankton Res., 14(8), 1129–1154, doi:10.1093/plankt/14.8.1129, 1992.

Andersen, V., Sardou, J. and Nival, P.: The diel migrations and vertical distributions of zooplankton and micronekton in the Northwestern Mediterranean Sea. 2. Siphonophores, hydromedusae and pyrosomids, J. Plankton Res., 14(8), 1155–1169, doi:10.1093/plankt/14.8.1155, 1992.

Andersen, V., Nival, P., Caparroy, P. and Gubanova, A.: Zooplankton community during the transition from spring bloom to oligotrophy in the open NW Mediterranean and effects of wind events. 1. Abundance and specific composition, J. Plankton Res., 23(3), 227–242, doi:10.1093/plankt/23.3.227, 2001.

Ashjian, C. J., Smith, S. L., Flagg, C. N. and Idrisi, N.: Distribution, annual cycle, and vertical migration of acoustically derived biomass in the Arabian Sea during 1994–1995, Deep Sea Res. Part II Top. Stud. Oceanogr., 49(12), 2377–2402, doi:10.1016/S0967-0645(02)00041-3, 2002.

Bozzano, R., Fanelli, E., Pensieri, S., Picco, P. and Schiano, M. E.: Temporal variations of zooplankton biomass in the Ligurian Sea inferred from long time series of ADCP data, Ocean Sci., 10(1), 93–105, doi:10.5194/os-10-93-2014, 2014.

Brierley, A. S., Brandon, M. A. and Watkins, J. L.: An assessment of the utility of an acoustic Doppler current profiler for biomass estimation, Deep Sea Res. Part I Oceanogr. Res. Pap., 45(9), 1555–1573, doi:10.1016/S0967-0637(98)00012-0, 1998.

Buesseler, K. O. and Boyd, P. W.: Shedding light on processes that control particle export and flux attenuation in the twilight zone of the open ocean, Limnol. Oceanogr., 54(4), 1210-1232, 2009.

Cardin, V., Gačić, M., Nittis, K., Kovačević, V. and Perini, L.: Sub-inertial variability in the Cretan Sea from the M3A buoy, Ann. Geophys., 21(1), 89–102, doi:10.5194/angeo-21-89-2003, 2003.

CDO: Climate Data Operators, [online] Available from: www.mpimet.mpg.de/cdo, 2018.

Cohen, J. H. and Forward, R. B.: Zooplankton diel vertical migration – A review of proximate control. Oceanogr. Mar. Biol. Ann. Rev., 47, 77-110, doi: 10.1201/9781420094220.ch2, 2009.

Costello, J. H., Pieper, R. E. and Holliday, D. V.: Comparison of acoustic and pump sampling techniques for the analysis of zooplankton distributions, J. Plankton Res., 11(4), 703–709, doi:10.1093/plankt/11.4.703, 1989.

Crise, A., Allen, J. I., Baretta, J., Crispi, G., Mosetti, R. and Solidoro, C.: The Mediterranean pelagic ecosystem response to physical forcing, Prog. Oceanogr., 44(1–3), 219–243, doi:10.1016/S0079-6611(99)00027-0, 1999.

Deines, K. L.: Backscatter estimation using Broadband acoustic Doppler current profilers, in: Proceedings of the IEEE 6th Working Conference on Current Measurement, San Diego, USA, 11-13 March 1999, 249–253,1999.

D'Ortenzio, F. and Ribera d'Alcalà, M.: On the trophic regimes of the Mediterranean Sea: a satellite analysis, Biogeosciences, 6(4), 139–148, doi:10.5194/bgd-5-2959-2008, 2009.

Flagg, C. N. and Smith, S. L.: On the use of the acoustic Doppler current profiler to measure zooplankton abundance, Deep Sea Res. Part A. Oceanogr. Res. Pap., 36(3), 455–474, doi:10.1016/0198-0149(89)90047-2, 1989.

Forward R. B.: Diel vertical migration: Zooplankton photobiology and behaviour, Oceanogr. Mar. Biol. Ann. Rev., 26, 361-393, 1988.

Fragopoulu, N. and Lykakis, J. J.: Vertical distribution and nocturnal migration of zooplankton in relation to the development of the seasonal thermocline in Patraikos Gulf, Mar. Biol., 104(3), 381–387, doi:10.1007/BF01314340, 1990.

Frangoulis, C., Christou, E. D. and Hecq, J. H.: Comparison of Marine Copepod Outfluxes: Nature, Rate, Fate and Role in the Carbon and Nitrogen Cycles, Adv. Mar. Biol., 47, 253–309, doi:10.1016/S0065-2881(04)47004-7, 2004.

Georgopoulos, D., Chronis, G., Zervakis, V., Lykousis, V., Poulos, S. and Iona, A.: Hydrology and circulation in the Southern Cretan Sea during the CINCS experiment (May 1994–September 1995), Prog. Oceanogr., 46(2–4), 89–112, doi:10.1016/S0079-6611(00)00014-8, 2000.

Gertman, I., Pinardi, N., Popov, Y. and Hecht, A.: Aegean Sea Water Masses during the Early Stages of the Eastern Mediterranean Climatic Transient (1988–90), J. Phys. Oceanogr., 36(9), 1841–1859, doi:10.1175/JPO2940.1, 2006.

Gordon, R.: Acoustic Doppler Currrent Profiler: Principles of operation, a practical primer, 2nd ed., Teledyne RD Instruments Inc., San Diego, California, USA. [online] Available from: http://misclab.umeoce.maine.edu/boss/classes/SMS_598_2012/RDI_Broadband Primer_ADCP.pdf, 1996.

Gotsis-Skretas, O., Pagou, K., Moraitou-Apostolopoulou, M. and Ignatiades, L.: Seasonal horizontal and vertical variability in primary production and standing stocks of phytoplankton and zooplankton in the Cretan Sea and the Straits of the Cretan Arc (March 1994–January 1995), Prog. Oceanogr., 44(4), 625–649, doi:10.1016/S0079-6611(99)00048-8, 1999.

Henson, S. A., Beaulieu, C. and Lampitt, R.: Observing climate change trends in ocean biogeochemistry: when and where, Glob. Chang. Biol., 22(4), 1561–1571, doi:10.1111/gcb.13152, 2016.

Heywood, K. J.: Diel vertical migration of zooplankton in the Northeast Atlantic, J. Plankton Res., 18(2), 163–184, doi:10.1093/plankt/18.2.163, 1996.

Holliday, D. V: Extracting bio-physical information from the acoustic signatures of marine organisms, in: Oceanic Sound Scattering Prediction, vol. 5, Plenum Press, New York, USA, 619–624, 1977.

Holliday, D. V and Pieper, R. E.: Volume scattering strengths and zooplankton distributions at acoustic frequencies between 0.5 and 3 MHz, J. Acoust. Soc. Am., 67(1), 135–146, doi:10.1121/1.384472, 1980.

Holliday, D. V, Pieper, R. E. and Kleppel, G. S.: Determination of zooplankton size and distribution with multifrequency acoustic technology, ICES J. Mar. Sci., 46(1), 52–61, doi:10.1093/icesjms/46.1.52, 1989.

Isla, A., Scharek, R. and Latasa, M.: Zooplankton diel vertical migration and contribution to deep active carbon flux in the NW Mediterranean, J. Mar. Syst., 143, 86-97, doi: 10.1016/j.jmarsys.2014.10.017, 2015.

Jiang, S., Dickey, T. D., Steinberg, D. K. and Madin, L. P.: Temporal variability of zooplankton biomass from ADCP backscatter time series data at the Bermuda Testbed Mooring site, Deep Sea Res. Part I Oceanogr. Res. Pap., 54(4), 608–636, doi:10.1016/j.dsr.2006.12.011, 2007.

Kassis, D., Korres, G., Petihakis, G. and Perivoliotis, L.: Hydrodynamic variability of the Cretan Sea derived from Argo float profiles and multi-parametric buoy measurements during 2010–2012, Ocean Dyn., 65(12), 1585–1601, doi:10.1007/s10236-015-0892-0, 2015.

Koppelmann, R., Weikert, H., Halsband-Lenk, C. and Jennerjahn, T.: Mesozooplankton community respiration and its relation to particle flux in the oligotrophic eastern Mediterranean, Global Biogeochem. Cycles, 18(1039), 1–10, doi:10.1029/2003GB002121, 2004.

Korres, G., Ntoumas, M., Potiris, M. and Petihakis, G.: Assimilating Ferry Box data into the Aegean Sea model, J. Mar. Syst., 140, 59–72, doi:10.1016/j.jmarsys.2014.03.013, 2014.

Koulouri, P., Dounas, C., Radin, F. and Eleftheriou, A.: Near-bottom zooplankton in the continental shelf and upper slope of Heraklion Bay (Crete, Greece, Eastern Mediterranean): observations on vertical distribution patterns, J. Plankton Res., 31(7), 753–762, doi:10.1093/plankt/fbp023, 2009.

Lavigne, H., D'Ortenzio, F., Ribera D'Alcalà, M., Claustre, H., Sauzède, R. and Gacic M.: On the vertical distribution of the chlorophyll a concentration in the Mediterranean Sea: a basin-scale and seasonal approach, Biogeosciences, 12, 5021-5039, doi: 10.5194/bg-12-5021-2015, 2015.

Madin, L. P., Horgan, E. F. and Steinberg, D. K.: Zooplankton at the Bermuda Atlantic Time-series Study (BATS) station: diel, seasonal and interannual variation in biomass, 1994–1998, Deep Sea Res. Part II Top. Stud. Oceanogr., 48(8–9), 2063–2082, doi:10.1016/S0967-0645(00)00171-5, 2001.

Malanotte-Rizzoli, P., Artale, V., Borzelli-Eusebi, G. L., Brenner, S., Crise, A., Gacic, M., Kress, N., Marullo, S., Ribera D'Alcalà, M., Sofianos, S., Tanhua, T., Theocharis, A., Alvarez, M., Ashkenazy, Y., Bergamasco, A., Cardin, V., Carniel, S., Civitarese, G., D'Ortenzio, F., Font, J., Garcia-Ladona, E., Garcia-Lafuente, J. M., Gogou, A., Gregoire, M., Hainbucher, D., Kontoyannis, H., Kovacevic, V., Kraskapoulou, E., Kroskos, G., Incarbona, A., Mazzocchi, M. G., Orlic, M., Ozsoy, E., Pascual, A., Poulain, P. M., Roether, W., Rubino, A., Schroeder, K., Siokou-Frangou, J., Souvermezoglou, E., Sprovieri, M., Tintoré, J. and Triantafyllou, G.: Physical forcing and physical/biochemical variability of the Mediterranean Sea: A review of unresolved issues and directions for future research, Ocean Sci., 10(3), 281–322, doi:10.5194/os-10-281-2014, 2014.

Mann, K. H. and Lazier, J. R. N.: Dynamics of Marine Ecosystems, Blackwell Scientific Publications Inc., USA., 2006.

Mazzocchi, G. M., Christou, E. D., Fragopoulu, N. and Siokou-Frangou, I.: Mesozooplankton distribution from Sicily to Cyprus (eastern Mediterranean): 1. General aspects, Oceanol. Acta, 20(3), 521–535, 1997.

Moriarty, R. and O'Brien, T. D.: Distribution of mesozooplankton biomass in the global ocean, Earth Syst. Sci. Data, 5(1), 45–55, doi:10.5194/essd-5-45-2013, 2013.

Nowaczyk, A., Carlotti, F., Thibault-Botha, D. and Pagano, M.: Distribution of epipelagic metazooplankton across the Mediterranean Sea during the summer BOUM cruise, Biogeosciences, 8(8), 2159–2177, doi:10.5194/bg-8-2159-2011, 2011.

Petihakis, G., Triantafyllou, G., Allen, I. J., Hoteit, I. and Dounas, C.: Modelling the spatial and temporal variability of the Cretan Sea ecosystem, J. Mar. Syst., 36(3–4), 173–196, doi:10.1016/S0924-7963(02)00186-0, 2002.

Pinot, J. M. and Jansá, J.: Time variability of acoustic backscatter from zooplankton in the Ibiza Channel (western Mediterranean), Deep Sea Res. Part I Oceanogr. Res. Pap., 48(7), 1651–1670, doi:10.1016/S0967-0637(00)00095-9, 2001.

Postel, L., da Silva, A. J., Mohrholz, V. and Lass, H.-U.: Zooplankton biomass variability off Angola and Namibia investigated by a lowered ADCP and net sampling, J. Mar. Syst., 68(1–2), 143–166, doi:10.1016/j.jmarsys.2006.11.005, 2007.

Razouls, C., de Bovée, F., Kouwenberg, J. and Desreumaux, N.: Diversity and Geographic Distribution of Marine Planktonic Copepods, [online] Available from: http://copepodes.obs-banyuls.fr/en/index.php, 2018.

Ringelberg, J.: Diel vertical migration of zooplankton in lakes and oceans: causal explanations and adaptive significances, Springer Netherlands, Dordrecht., 2010.

Robinson, C., Steinberg, D. K., Anderson, T. R., Arístegui, J., Carlson, C. A., Frost, J. R., Ghiglione, J.-F., Hernández-León, S., Jackson, G. A., Koppelmann, R., Quéguiner, B., Ragueneau, O., Rassoulzadegan, F., Robison, B. H., Tamburini, C., Tanaka, T., Wishner, K. F. and Zhang, J.: Mesopelagic zone ecology and biogeochemistry – a synthesis, Deep Sea Res. Part II Top. Stud. Oceanogr., 57(16), 1504–1518, doi:10.1016/j.dsr2.2010.02.018, 2010.

Saiz, E., Sabatés, A. and Gili, J.-M.: The Zooplankton, in: The Mediterranean Sea: Its history and present challenges, Springer Netherlands, Dordrecht, Netherlands, 183–211, 2014.

Sardou, J., Etienne, M. and Andersen, V.: Seasonal abundance and vertical distributions of macroplankton and micronekton in the Northwestern Mediterranean Sea, Oceanol. Acta, 19(6), 645–656, 1996.

Schlitzer, R.: Ocean Data View, [online] Available from: https://odv.awi.de, 2016.

Siokou-Frangou, I., Christou, E. D., Fragopoulu, N. and Mazzocchi, M. G.: Mesozooplankton distribution from Sicily to Cyprus (eastern Mediterranean): II. Copepod assemblages, Oceanol. Acta, 20(3), 537–548, 1997.

Siokou-Frangou, I., Christaki, U., Mazzocchi, M. G., Montresor, M., Ribera d'Alcalá, M., Vaqué, D. and Zingone, A.: Plankton in the open Mediterranean Sea: a review, Biogeosciences, 7(5), 1543–1586, doi:10.5194/bg-7-1543-2010, 2010.

Siokou, I., Zervoudaki, S. and Christou, E. D.: Mesozooplankton community distribution down to 1000 m along a gradient of oligotrophy in the Eastern Mediterranean Sea (Aegean Sea), J. Plankton Res., 35(6), 1313–1330, doi:10.1093/plankt/fbt089, 2013.

Skliris N.: Past, Present and Future Patterns of the Thermohaline Circulation and Characteristic Water Masses of the Mediterranean Sea. In: Goffredo S., Dubinsky Z. (eds) The Mediterranean Sea. Springer, Dordrecht, doi: 10.1007/978-94-007-6704-1_3, 2014.

Tedetti, M. and Sempéré, R.: Penetration of ultraviolet radiation in the marine environment. A review, Photochem. Photobiol., 82(2), 389-397, doi:10.1562/2005-11-09-IR-733, 2006.

Theocharis, A., Balopoulos, E., Kioroglou, S., Kontoyiannis, H. and Iona, A.: A synthesis of the circulation and hydrography of the South Aegean Sea and the Straits of the Cretan Arc (March 1994–January 1995), Prog. Oceanogr., 44(4), 469–509, doi:10.1016/S0079-6611(99)00041-5, 1999.

Thomson, R. E. and Emery, W. J.: Data Analysis Methods in Physical Oceanography, 2nd ed., Elsevier, USA, 2001.

Turner, J. T.: Zooplankton fecal pellets, marine snow, phytodetritus and the ocean's biological pump, Prog. Oceanogr., 130, 205–248, doi:10.1016/j.pocean.2014.08.005, 2015.

van Haren, H.: Internal wave–zooplankton interactions in the Alboran Sea (W-Mediterranean), J. Plankton Res., 36(4), 1124-1134, doi: 10.1093/plankt/fbu031, 2014.

Varela, R. A., Cruzado, A. and Tintoré, J.: A simulation analysis of various biological and physical factors influencing the deep-chlorophyll maximum structure in oligotrophic areas, J. Mar. Syst., 5(2), 143–157, doi:10.1016/0924-7963(94)90028-0, 1994.

Velaoras, D., Krokos, G. and Theocharis, A.: An internal mechanism alternatively drives the preconditioning of both the Adriatic and Aegean Seas as dense water formation sites in the Eastern Mediterranean, Rapp. Comm. Int. Mer Medit., 40, 178, 2013.

Velaoras, D., Krokos, G. and Theocharis, A.: Recurrent intrusions of transitional waters of Eastern Mediterranean origin in the Cretan Sea as a tracer of Aegean Sea dense water formation events, Prog. Oceanogr., 135, 113–124, doi:10.1016/j.pocean.2015.04.010, 2015.

Wiebe, P. H. and D'Abramo, L: Distribution of euphausiid assemblages in the Mediterranean Sea, Mar. Biol., 15, 139-149, doi:10.1007/BF00353642, 1972.

Wessel, P., Smith, W. H. F., Scharroo, R., Luis, J. and Wobbe, F.: Generic Mapping Tools: Improved Version Released, Eos, Trans. Am. Geophys. Union, 94(45), 409–410, doi:10.1002/2013EO450001, 2013.

Williamson, C. E., Fischer J. M., Bollens S. M., Overholt E. P. and Breckenridge J. K.: Toward a more comprehensive theory of zooplankton diel vertical migration: Integrating ultraviolet radiation and water transparency into the biotic paradigm, Limnol. Oceanogr., 56, 1603-1623, doi: 10.4319/lo.2011.56.5.1603, 2011.

Zervakis, V., Georgopoulos, D. and Drakopoulos, P. G.: The role of the North Aegean in triggering the recent Eastern Mediterranean climatic changes, J. Geophys. Res. Ocean., 105(C11), 26103–26116, doi:10.1029/2000JC900131, 2000.

Zhou, M. and Dorland, R. D.: Aggregation and vertical migration behavior of Euphausia superba, Deep Sea Res. Part II Top. Stud. Oceanogr., 51(17–19), 2119–2137, doi:10.1016/j.dsr2.2004.07.009, 2004.

Table 1: The deployment parameters of the upward looking 75 kHz RDI ADCP on the subsurface mooring line of E1-M3A are listed.

Deployment	Start	End	Bins	Bin size (m)	Sampling interval (s)	1st Bin (m)	Average depth (m)
1st	15-Nov-2012	23-May-2013	25	16	1800	24.59	369
2nd	01-Jun-2013	19-Jan-2014	33	12	3600	20.65	383
3rd	19-Jan-2014	10-Oct-2014	25	20	1800	28.58	370
4th	10-Oct-2014	02-Jun-2015	45	10	1800	18.76	509

Table 2: The type, source, time coverage and resolution of the auxiliary data are listed. In situ data have gaps of variable length. Monitoring by R/V refers to the monthly monitoring program by regular R/V visits at the E1-M3A observatory site. NASA refers to the Goddard Space Flight Center.

Parameter	Type	Source	Time Coverage	Time Resolution
Air temp & wind	*In situ*	E1-M3A buoy	2013/05-2014/10	3 h
Surface currents (0-50 m)	*In situ*	E1-M3A buoy (ADCP 400kHz)	2013/05-2015/05	3 h
Subsurface currents (0-400 m)	*In situ*	ADCP (75kHz)	2012/11-2015/05	0.5-1 h
Water temp & sal	*In situ*	E1-M3A buoy	2013/05-2015/01	3 h
	In situ	Monitoring by R/V	2010/03-2015/01	1 m
	Reanalysis	SeaDataNet	Climatology	1 m
Chl-α	*In situ*	E1-M3A buoy	2013/05-2014/06	3 h
	In situ	Monitoring by R/V	2010/03-2015/05	1 m
Cloud fraction & optical thickness	Satellite	NASA	2015/02-2015/03	1 d

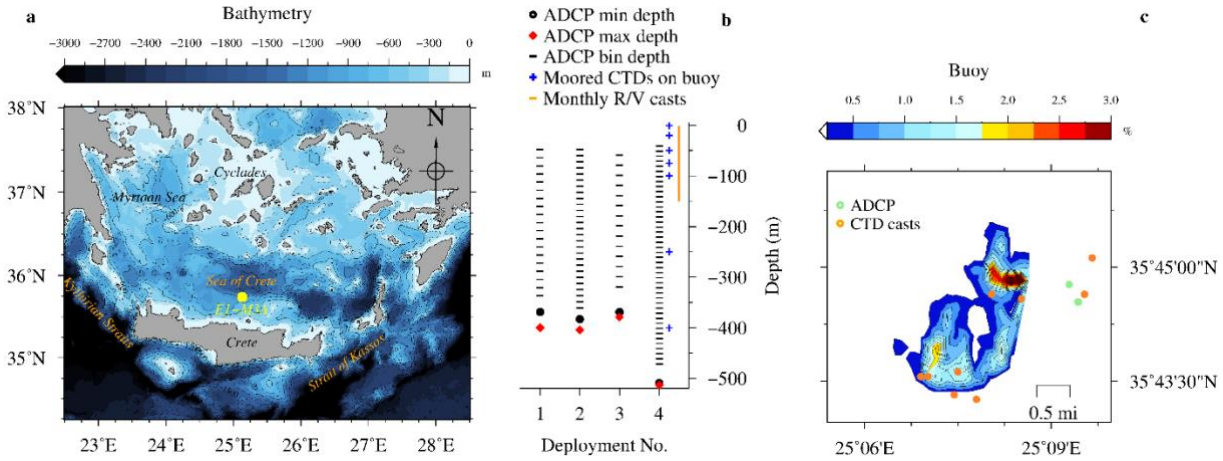

Figure 1: Topographic map of the south Aegean Sea (a), vertical (b) and horizontal (c) views of the sampling set up at E1-M3A. Details of ADCP deployments are given in Table 1. Horizontal buoy motion is shown as the percent of the time of total deployment duration spent at a location.

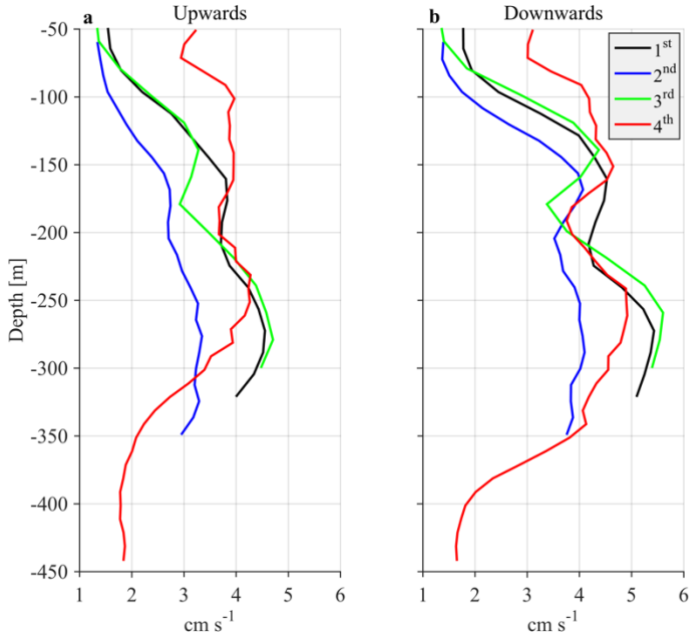

Figure 2: Time average burst speeds per ADCP deployment.

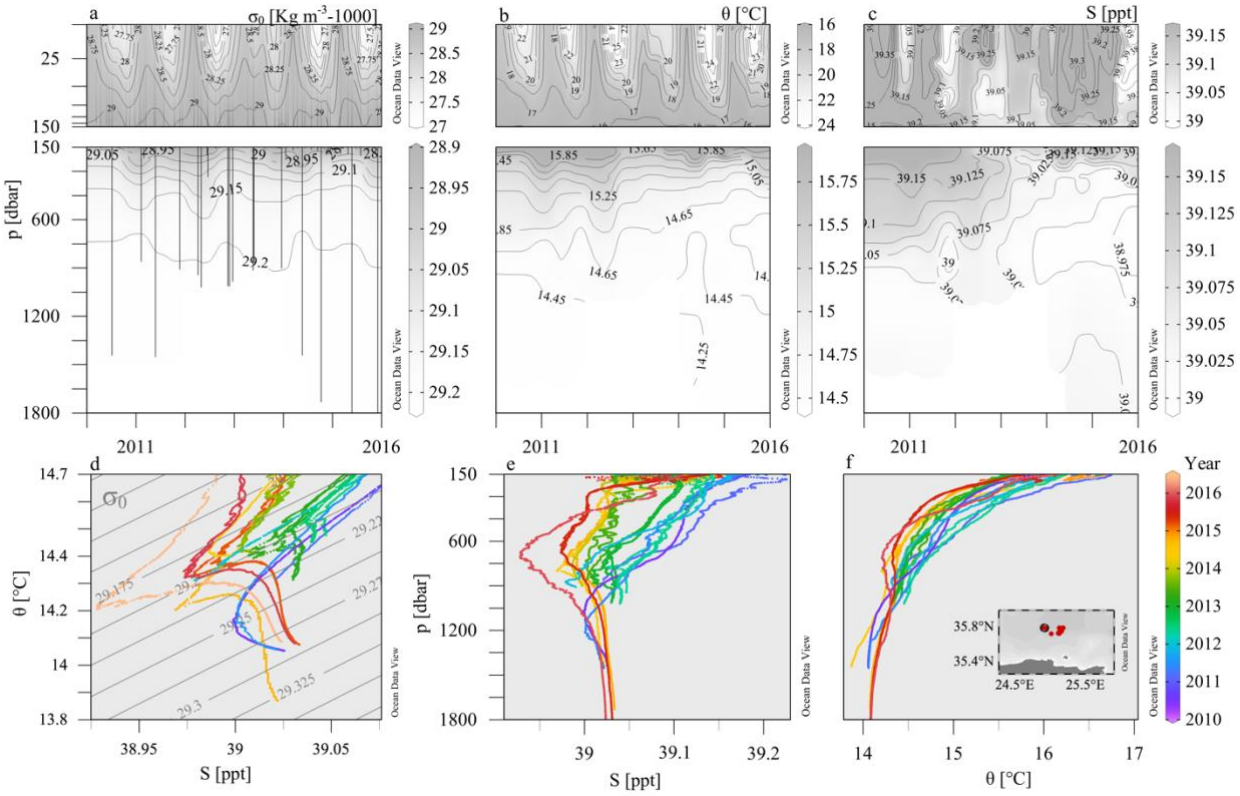

Figure 3: CTD casts collected during monitoring and maintenance visits at the site of E1-M3A observatory with HCMR research vessels from 2010 to 2016. Time-depth plots of potential density anomaly σ_0 (a), potential temperature θ (b) and practical salinity S (c). $\theta - S$ plot (d) and vertical profiles of S (e) and θ (f) are colored according to date to reveal temporal trends.

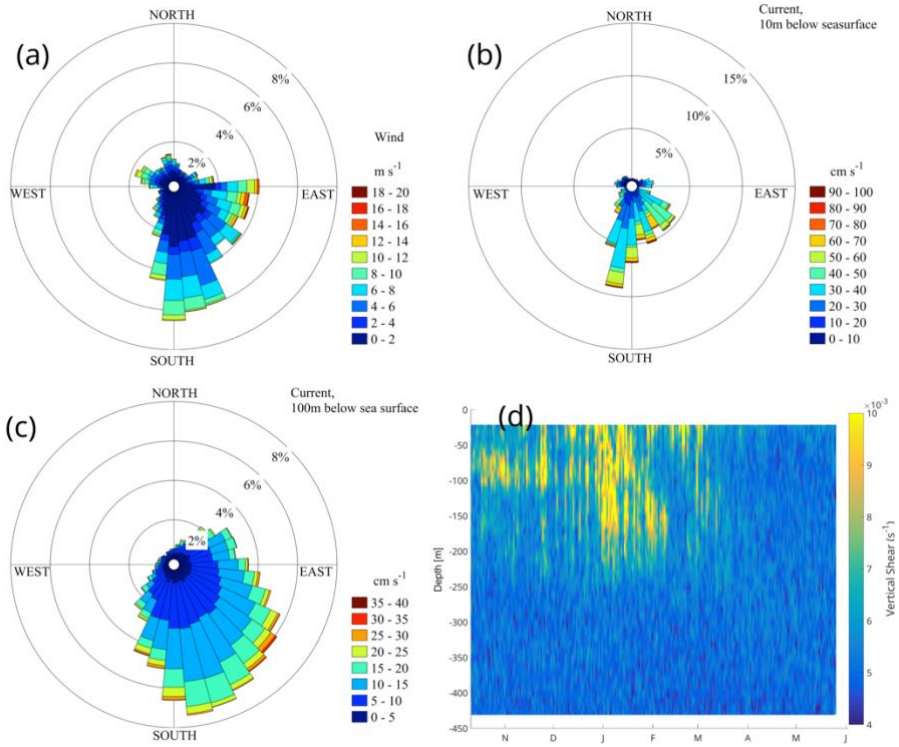

Figure 4: Rose diagrams of wind (a) and surface (10 m depth) currents from the buoy's ADCP (400 kHz downward looking) (b), subsurface currents at 100 m depth from the upward looking 75 kHz ADCP (c) and vertical shear from the fourth deployment (d). The direction in panels (a, b, c) point to the direction of the flow.

5

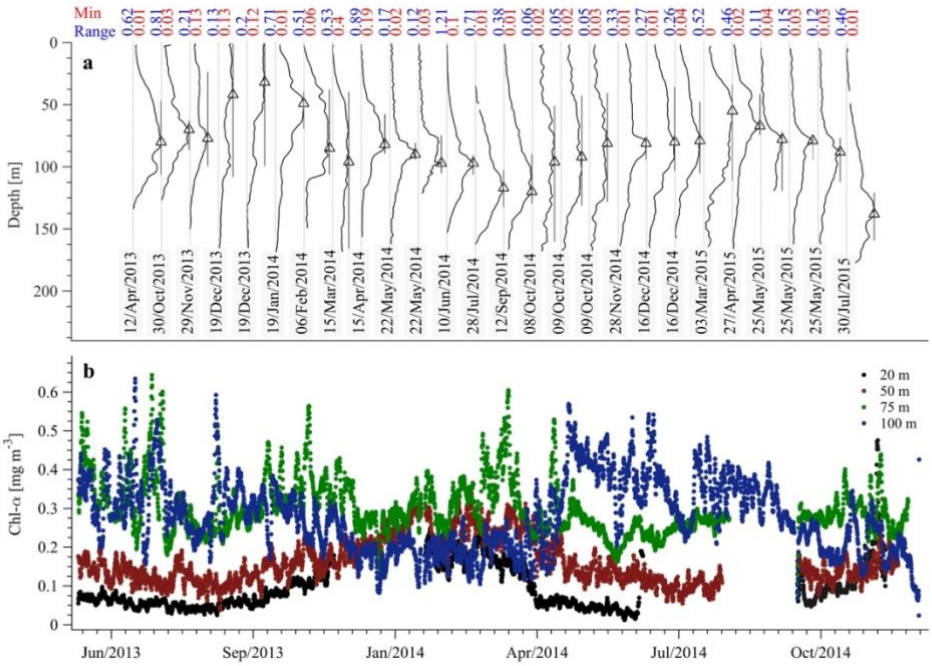

Figure 5: Chlorophyll concentration from the CTD casts (a) and E1-M3A CTD sensors (b). The casts show the vertical distribution of chlorophyll concentration in the water column (normalized, solid black lines). The minimum value of each cast is denoted by the vertical gray line and the maximum value of each cast is denoted by the black triangle. The gray bars around the triangles denote the depth range for which the chlorophyll concentration is above 70% of the maximum value of the cast. The minimum value and the range of original chlorophyll values (in mg m^{-3}) are shown above each cast in red and blue colors respectively. E1-M3A chlorophyll data are low passed with a one-day running mean filter.

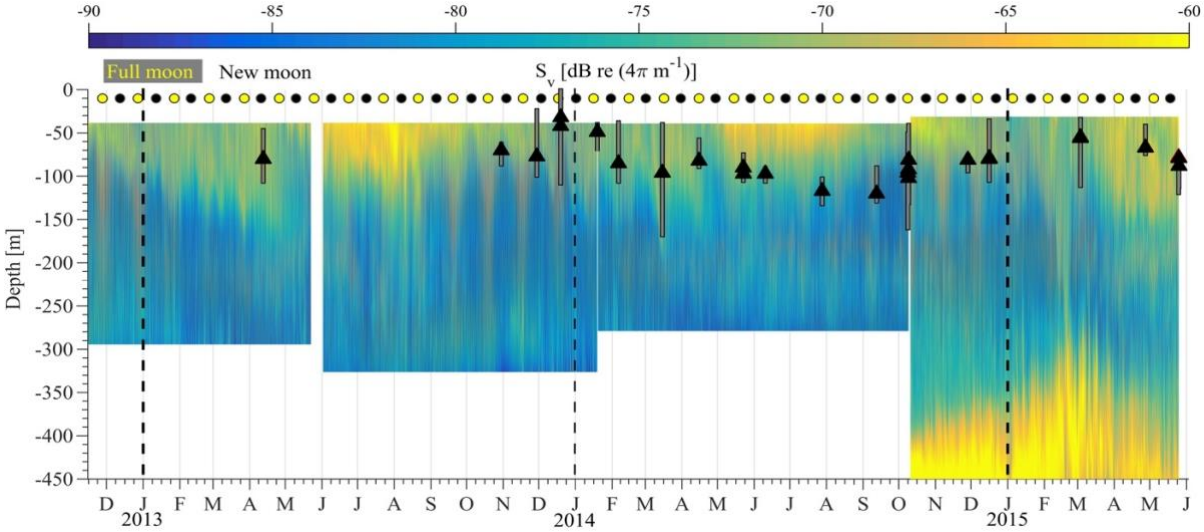

Figure 6: The backscatter coefficient for all ADCP deployments is shown. The beginning of a year is denoted by the dashed vertical line. The yellow and black circles denote the dates of full moon and new moon respectively. The maximum chlorophyll value of available casts is denoted by the black triangle. The gray bars around the triangles denote the depth range for which the chlorophyll concentration is above 70% of the maximum value of the cast.

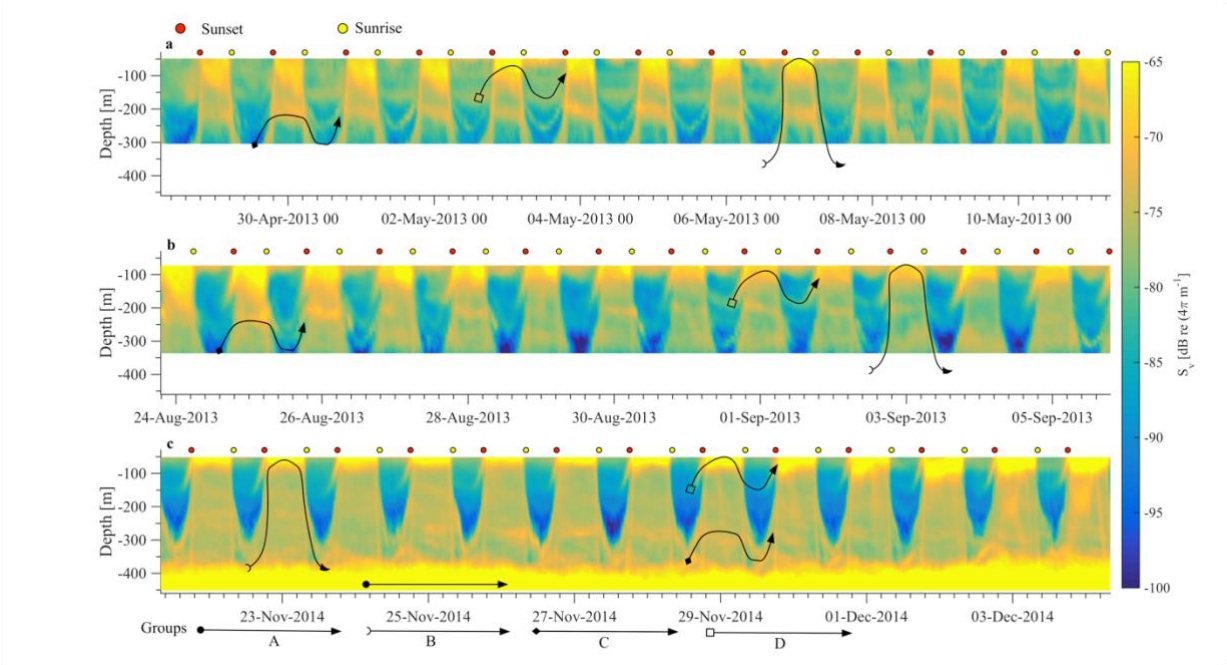

Figure 7: Hand drawn trails of S_v attributed to groups of planktonic and micro-nectonic organisms.

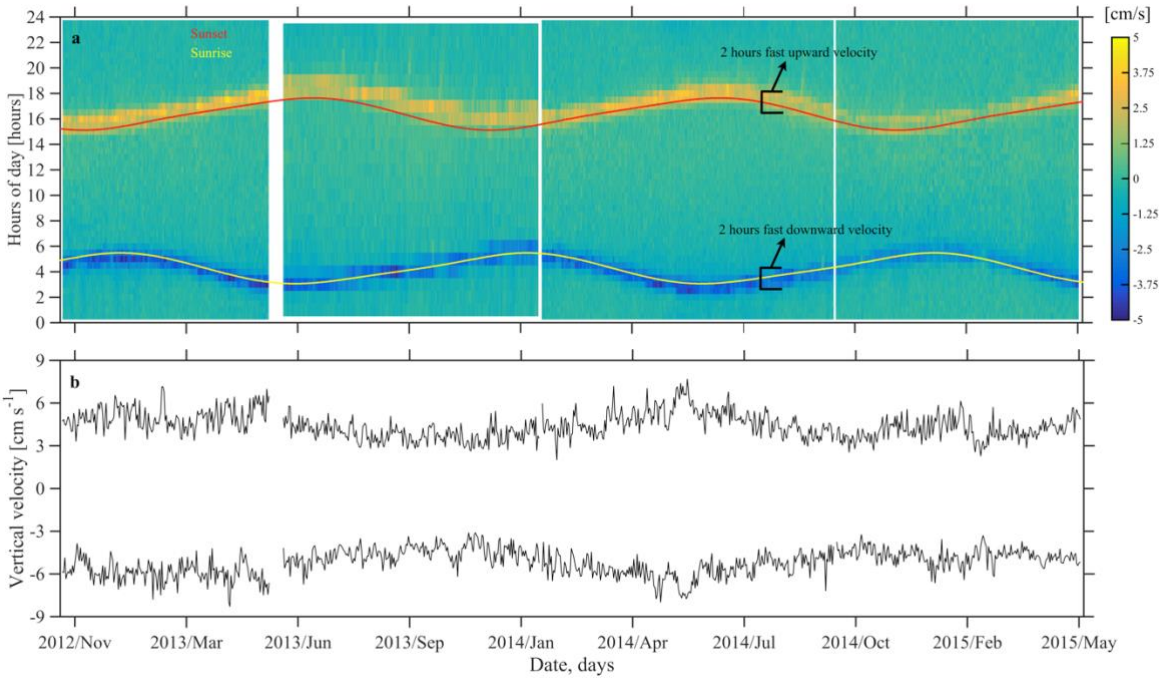

Figure 8: (a) Instantaneous depth averaged vertical velocities of daily segments of ADCP measurements between 350 m and 50 m, following Jiang et al. (2007). Sunrise and sunset times are superimposed. (b) Average of the three highest upwards and downwards velocity values per day. The hours of fast zooplankton motion are also shown.

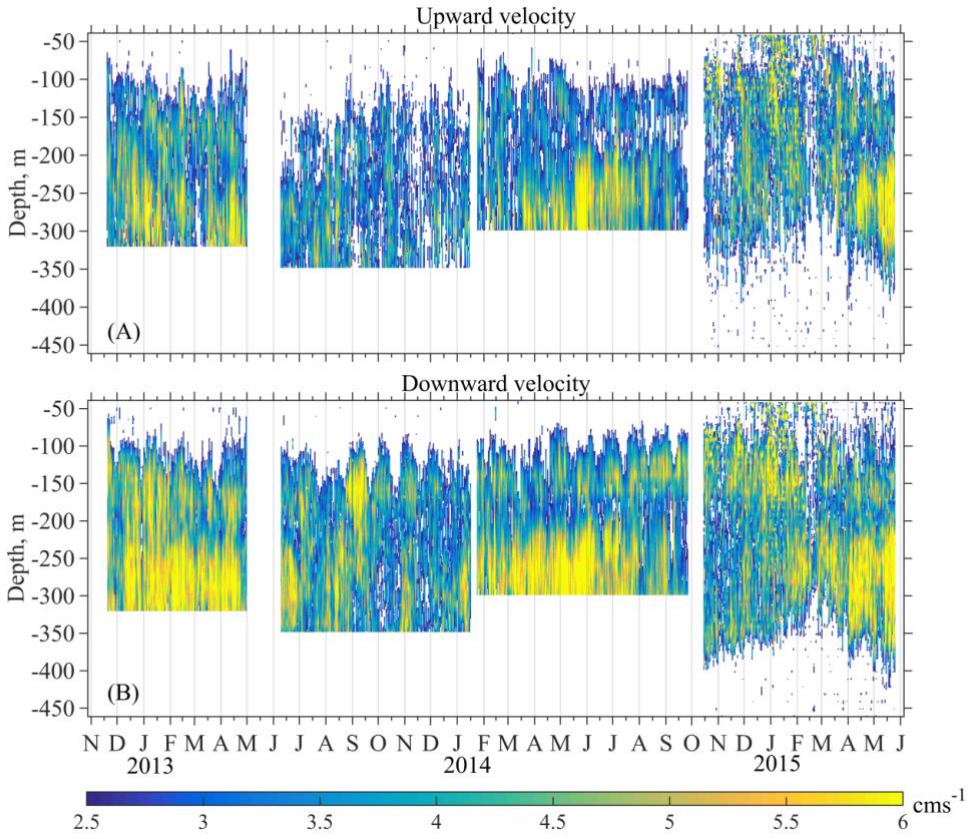

Figure 9: Large upwards (A) and downwards (B) velocity, attributed to the migration of zooplankton.

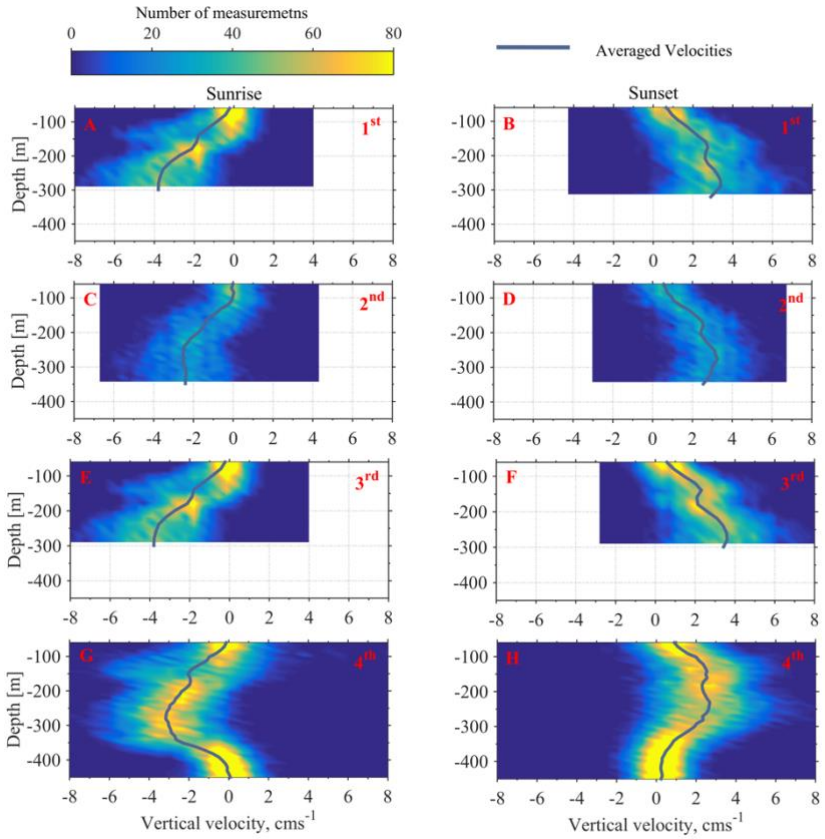

Figure 10: Depth distributions of the vertical velocities, measured 1 h before and 1 h after sunset and sunrise, are shown. The time average velocity at each depth is superimposed. Each row of panels refers to one deployment (1st, 2nd, 3rd, 4th). The first column of panels corresponds to sunrise and the second column to sunset.

5

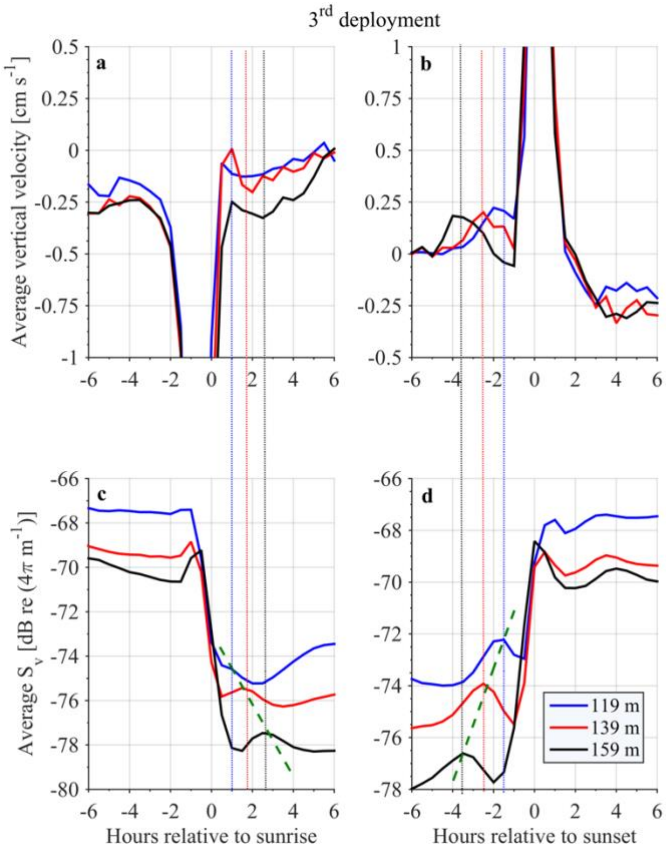

Figure 11: Time average vertical velocity (a, b) and S_v (c, d) at selected depths during the 3rd deployment. The green dashed line connects the S_v peaks attributed to group D. The vertical dotted lines are used to facilitate the common vertical velocity and S_v peaks, attributed to group D.

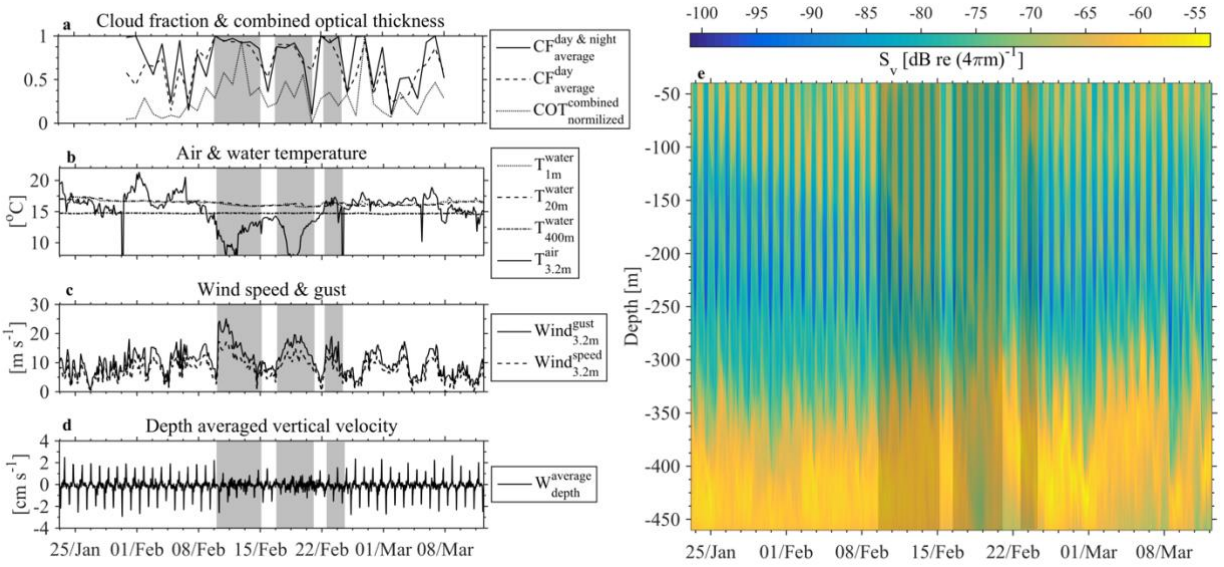

Figure 12: Cloudiness (a), air and water temperature (b) and wind conditions (c) are examined in comparison to depth averaged vertical velocities (d) and backscatter coefficient (e) during February 2015. Gray shaded areas denote the three harsh weather events referred in the text.

5